Taylor & Francis
Taylor & Francis Group

Pharmaceutical Development and Technology

ISSN: 1083-7450 (Print) 1097-9867 (Online) Journal homepage: https://www.tandfonline.com/loi/iphd20

A Promising Approach to Develop Nanostructured Lipid Carriers from Solid Lipid Nanoparticles: Preparation, Characterization, Cytotoxicity and Nucleic Acid Binding Ability

Ezgi Oner, Mustafa Kotmakci & Ayse Gulten Kantarci

To cite this article: Ezgi Oner, Mustafa Kotmakci & Ayse Gulten Kantarci (2020): A Promising Approach to Develop Nanostructured Lipid Carriers from Solid Lipid Nanoparticles: Preparation, Characterization, Cytotoxicity and Nucleic Acid Binding Ability, Pharmaceutical Development and Technology, DOI: 10.1080/10837450.2020.1759630

To link to this article: https://doi.org/10.1080/10837450.2020.1759630

Accepted author version posted online: 21 Apr 2020.

A Promising Approach to Develop Nanostructured Lipid Carriers from Solid Lipid Nanoparticles: Preparation, Characterization, Cytotoxicity and Nucleic Acid Binding Ability

Ezgi Oner[a], Mustafa Kotmakci[a], Ayse Gulten Kantarci[a]*

[a]*Department of Pharmaceutical Biotechnology, Faculty of Pharmacy, Ege University, Izmir, Turkey.*

*E-mail: gulten.kantarci@ege.edu.tr. Address: Ege University, Faculty of Pharmacy, Department of Pharmaceutical Biotechnology, Campus Bornova, 35100, Izmir, Turkey. Phone: +90 232 311 25 75.

A Promising Approach to Develop Nanostructured Lipid Carriers from Solid Lipid Nanoparticles: Preparation, Characterization, Cytotoxicity and Nucleic Acid Binding Ability

We aimed to develop nanostructured lipid carriers (NLCs) displaying similar characteristics- particle size, polydispersity index, and zeta potential- with the model solid lipid nanoparticles (SLNs) for better comparability. By considering the hydrophilic-lipophilic balance (HLB) values of solid and liquid lipids, five out of six NLCs and eight out of eight cationic NLCs (cNLCs) were successfully prepared with similar characteristics to their precursor SLN and cationic SLNs (cSLNs), respectively. Among cationic formulations, two cSLNs containing different surfactant/co-surfactant concentrations (4% and 8% S/CoS; w/w) and their cNLC versions prepared with Labrafac lipophile WL 1349 (LWL) or Labrafac PG were selected to compare cytotoxicity, stability, and nucleic acid binding ability. All formulations are well-tolerated by L-929 cells, cSLNs being least toxic. The formulations containing 4% S/CoS had higher stability after 24-months. All nanoparticles formed complexes with pDNA (Binding ability: cNLCs>cSLNs). cSLN and LWL-cNLC containing 4% S/CoS showed the highest pDNA binding capacity in each group, and their spherical/oval shape was revealed by electron microscopy. However, they did not form complexes with siRNA. The developed approach has the potential to simplify the production of (c)NLCs having similar physicochemical properties with the optimum (c)SLN and may provide better insight for (c)SLN *vs.* (c)NLC comparison studies.

Keywords: solid lipid nanoparticles; SLN; nanostructured lipid carriers; NLC; cytotoxicity; nucleic acid delivery; plasmid DNA; siRNA; Labrafac lipophile WL 1349; Labrafac PG.

Introduction

For more than a decade, research in the drug delivery field has focused considerably on the development of nanoparticulate delivery systems (Park 2014). Nanoparticles are widely investigated for targeted delivery of poorly soluble small molecule drugs and to enable the delivery of nucleic acids for gene therapy (Park 2014; Gupta et al. 2017). Currently, many nanoparticle formulations are under investigation in clinical trials, and some of them have been approved for clinical use (Anselmo & Mitragotri 2016). Among nanoparticle systems, lipid nanoparticles with solid matrix have gained attention as an alternative to liposomes, nanoemulsions, and polymer-based nanoparticles (Sánchez-López et al. 2017; Teixeira et al. 2017). These lipid nanoparticles are mainly classified as solid lipid nanoparticles (SLNs) and nanostructured lipid carriers (NLCs) (Naseri et al. 2015).

In the early 1990s, SLNs were first developed using solid lipids, which are solid at body and room temperature (Gasco 1991; H. Muller et al. 2011). SLNs are considered as promising carriers due to their potential advantages such as (i) low toxicity due to biocompatibility and biodegradability, (ii) preparation without need of organic solvents, (iii) suitability for large-scale manufacturing, (iv) easy encapsulation of highly lipophilic drugs, (v) enhanced stability of encapsulated molecules due to lipid matrix shielding, (vi) ease of surface modification for targeting purposes, (vii) co-delivery of lipophilic drugs and nucleic acids by adding cationic lipids in the composition (Das et al. 2012; Shah et al. 2015). However, solid lipids in the structure of SLNs may display polymorphic transitions during storage (Sánchez-López et al. 2017). These solid lipids in SLNs remain mostly in a high-energy (thermodynamically unstable) α form after preparation. Upon storage, α crystalline form of lipids converts to a low-energy β form, which leads to a more ordered crystal matrix (*i.e.* a decrease in

imperfection). Even if the SLNs initially display desired characteristics the more ordered crystal matrix leads to drawbacks such as low storage stability and drug leakage from the matrix (Müller et al. 2000; Mehnert & Mader 2002; Sánchez-López et al. 2017). To minimize these drawbacks, NLCs were evolved from SLNs in 1999 as the second generation lipid nanoparticles (H. Muller et al. 2011; Sánchez-López et al. 2017). NLCs contain liquid lipid(s) as well as solid lipid(s) in their composition. The presence of liquid lipids increases the imperfections in the crystal solid matrix, which leads to the superiority of NLCs over SLNs (Das & Chaudhury 2011; Kovacevic et al. 2011; Khalil et al. 2014).

Many researchers investigate SLNs and NLCs, and compare these delivery systems in terms of cytotoxicity (Ruktanonchai et al. 2009; Dong et al. 2009; Fang et al. 2011), stability (Souto et al. 2004a; Souto et al. 2004b; Das et al. 2012; Tosta et al. 2014; Kelidari et al. 2017), drug loading capacity (Souto et al. 2004a; Das et al. 2012; Tosta et al. 2014; Balguri et al. 2016; Kelidari et al. 2017), drug release (Souto et al. 2004a; Fang et al. 2011; Das et al. 2012; Tosta et al. 2014; Balguri et al. 2016), drug expulsion during storage (Das et al. 2012), *etc.* In these studies, NLCs are generally prepared from the SLN formulations by partially replacing the solid lipid with the same amount of a liquid lipid. However, the type and amount of liquid lipids in NLCs are determined empirically (Souto et al. 2004a; Lombardi Borgia et al. 2005) or by selecting among several tested formulations (Souto et al. 2004b; Dong et al. 2009; Kovacevic et al. 2011; Balguri et al. 2016; Kelidari et al. 2017). This causes NLCs to display distinct physicochemical properties as compared to their model SLNs (Fang et al. 2011; Bahari & Hamishehkar 2016; Kelidari et al. 2017) and these differences result in variations in their activities, both *in vitro* and *in vivo* (Dong et al. 2009; Hoshyar et al. 2016; Lundy et al. 2016). To eliminate these variations related to differences in

physicochemical properties, we suggest that using a previously characterized SLN formulation as a model to develop NLCs with similar size, size distribution, and zeta potential may provide better insight for comparison of both nanoparticle types. Also, developing these NLCs as a 'superior' alternative to the model SLN- having desirable characteristics, but also some drawbacks because of its perfect crystalline matrix- may be useful in the formulation optimization process.

Therefore, this study aimed to develop an approach for obtaining NLCs with similar physicochemical properties to a previously established SLN by keeping equal hydrophilic-lipophilic balance (HLB) value for liquid and solid lipids. Moreover, while NLCs are generally known as a better choice for the delivery of small-molecule drugs than SLNs, little is known about their nucleic acid complexation capability as compared to SLNs. As such, we applied this approach also to develop cationic NLCs (cNLCs) from cationic SLNs (cSLNs) to compare their nucleic acid [plasmid DNA (pDNA) and small interfering RNA (siRNA)] binding ability in addition to cytotoxicity and storage stability.

Materials and methods

Materials

Solid lipids Precirol ATO 5 (P), Compritol 888 ATO (C); liquid lipids Labrafac lipophile WL 1349 (LWL), Labrafac PG (LPG), Lauroglycol 90 (L90), Capryol PGMC (PGMC) were all generous gifts from Gattefossé (France). As surfactants; Kolliphor RH 40 (Cremophor RH 40, KRH40) was a kind gift from BASF (Germany), Span 80 (S80) was purchased from Sigma-Aldrich (Germany). Propylene glycol (PG) used as co-surfactant was acquired from Merck (Germany). Cationic lipids; Esterquat-1 [EQ1, N-(β-Palmitoylethyl)-N-(β-stearoylethyl)-N,N-dimethyl-ammonium chloride] was from

GERBU Biotechnik GmbH (Germany) and dimethyldioctadecylammonium bromide (DDAB) was from Tokyo Chemical Industry (Japan). Ultra-pure water (upH_2O) was used in all formulations. More detail about these ingredients is provided in **Supplementary Table 1**.

Dulbecco's Modified Eagle's Medium (DMEM, #41965-039), fetal bovine serum (FBS; #10270-106), 0.25% Trypsin-EDTA (#25200-056) and penicillin/streptomycin solution (P/S; #15140-122) were purchased from Gibco. The pDNA (pSIH1-puro-control shRNA) was a gift from Frank Sinicrope (Addgene plasmid # 26597) (Huang & Sinicrope 2010) and siRNA targeting human EphA2 receptor (ON-TARGETplus SMARTpool; #L-003116-00-0020) was purchased from Dharmacon (USA).

Preparation of nanoparticles

Composition of (c)SLN and (c)NLC formulations

The compositions of SLNs and their cationic forms (cSLNs) are provided in **Table 1**.

While determining the composition of (c)NLCs derived from (c)SLNs, the percentage of total lipid was not changed; *i.e.* the solid lipids (SLs) were replaced with the liquid lipids (LLs) at two different SL:LL ratios, 3:2 and 3.5:1.5. We selected these ratios among the preferred SL:LL ratios ranging from 70:30 to 99.9:0.1 (Khosa et al. 2018), which successfully formed NLCs containing oils in a solid matrix previously (Khalil et al. 2014; Song et al. 2016). Also, the HLB values of both lipids was kept constant using **Equation 1**.

Total HLB value of SLs in (c)SLN = Total HLB value of SLs and LLs in (c)NLC (1)

$$(\%\ SL1 \times HLB_{SL1} + \%\ SL2 \times HLB_{SL2} =$$

$$\%\ SL1 \times HLB_{SL1} + \%\ SL2 \times HLB_{SL2} + \%\ LL1 \times HLB_{LL1} + \%\ LL2 \times HLB_{LL2})$$

where, % SL or % LL is the percentage of the lipid in the formulation (w/w) and HLB is the theoretical hydrophilic-lipophilic balance value of the lipid provided by the manufacturer. According to this, the compositions of NLCs and their cationic forms (cNLCs) are provided in **Table 2**.

Preparation of nanoparticles by modified hot microemulsion method

All of the formulations were prepared by slightly modifying the hot microemulsion stepwise method in a previous study carried out in our laboratory (Kotmakçı et al. 2016). Firstly, stocks were prepared for both the mixture of surfactants & co-surfactant (S/CoS) and the mixture of solid lipids (or liquid lipids). All ingredients, except upH_2O, were weighed into a 4 mL glass vial. This mixture was stirred in a heating jacket at 80°C (above the melting points of solid lipids) by a magnetic stirrer (MTOPS- HSD180, Misung Scientific, Korea) until a homogenous mixture was obtained (2 min, 1500 rpm). Ultra-pure water, placed in the heating jacket at 80°C, was added dropwise to the mixture with P200 micropipette (8 min, 1500 rpm). After water addition, the vial was immediately taken from the heating jacket and stirred at room temperature (30 min, 1500 rpm).

Preparation of complexes and nucleic acid binding assay (gel shift assay)

Complex formation is based on the electrostatic interactions between positively charged nanoparticles and negatively charged nucleic acids (pDNA, siRNA, *etc.*). The binding ability of cationic nanoparticles to pDNA and siRNA was determined by agarose gel electrophoresis (MyGel mini electrophoresis system, Sigma). **Equation 2** was used to determine the optimum N/P ratio (the molar ratio of the cationic lipid nitrogens to nucleic acid phosphates) for each formulation to bind pDNA and siRNA:

(2)

$$(\mathrm{N/P}) = \frac{\text{Volume of cSLN or cNLC (µL) x EQ1 concentration in cSLN or cNLC (mM)}}{\text{Weight of the pDNA or siRNA (µg) x Phosphate } \left(\frac{\text{nmol}}{\text{µg}}\right)}$$

where, the densities of all formulations were assumed as 1 g/mL and 1 µg of the pDNA or siRNA equals 3 nmol of phosphate (Barichello et al. 2010). An example for the calculation of N/P ratio is provided in the **Supplementary Data**.

The required volume of the formulation to form complex with pDNA (200 ng) or siRNA (67 ng) was calculated according to desired N/P ratio. After adding the required volumes of formulation, either pDNA or siRNA and diluent (upH_2O or PBS) to a final volume of 18 µL, this mixture was incubated on a shaker (IKA vortex genius 3, Germany) at room temperature (~1000 rpm, 30 min). Glycerol (50%, 2 µL) was added to each sample prior to loading on to agarose gels. pDNA samples were loaded on to 0.8 % agarose gel in 1X tris-acetate-EDTA (TAE) buffer and siRNA samples were loaded on to 2 % agarose gel in 0.5X tris-borate-EDTA (TBE) buffer. After electrophoresis (100 V, 15 or 20 min) (Yu et al. 2012), the gel was stained with 0.5 µg/mL ethidium bromide solution for 10 min following a washing step with distilled water for 2 min. Visualisation was then performed using a UV Transilluminator (Vilber Lourmat, France). Naked pDNA or siRNA was used as a control.

Measurement of particle size, polydispersity index, zeta potential and pH

Each formulation was diluted 10-fold and pDNA:nanoparticle complexes were diluted 40-fold in upH_2O prior to measurements. The Z-average particle size (D) and polydispersity index (PDI) were measured in disposable polystyrene microcuvettes by dynamic light scattering (DLS, also known as Photon Correlation Spectroscopy) technique at 173° back-scattering mode using Zetasizer NanoZS instrument (Malvern

Panalytical Ltd., UK). The electrophoretic mobility was measured with electrophoretic light scattering (ELS) technique in standard zeta cuvettes (Malvern Panalytical Ltd., UK) using the same instrument, and zeta potential (ZP) was calculated according to the Smoluchowski equation by the software. The measurements were carried out at 25°C at least in triplicate. All formulations were stored in 4 mL screw top & clear glass vials with polytetrafluoroethylene-lined caps (Agilent, USA) at room temperature for storage stability test.

The formulations were diluted 10-fold in PBS or upH_2O and their pH were measured by a pH meter with a microelectrode (SevenGo Duo SG23, Mettler Toledo, USA).

Differential scanning calorimetry (DSC)

The melting behavior of solid lipids was investigated using DSC Q20 (TA Instruments, USA) at Ege University Application and Research Center for Testing and Analysis (EGE-MATAL), Turkey. All samples (2-4 mg) were accurately weighed in the aluminum pans and hermetically sealed. Thermograms were obtained by heating the samples from 25°C to 90°C at 5°C/min heating rate under nitrogen gas using an empty sealed pan as a reference (Doktorovova et al. 2011). Onset temperature, melting point (T_{max}), and enthalpy values were calculated using TA Universal Analysis 2000 software (USA).

X-ray diffraction (XRD)

Time-dependent change in the crystallinity of the formulations was investigated using PANalytical Empyrean Alpha-1 X-Ray Diffractometer (Malvern Panalytical Ltd., UK) at Central Research Laboratory in Izmir Katip Celebi University, Turkey. XRD was performed at 2-theta (2θ) angle from 5° to 35° under continuous scan with a copper

anode (at 45 kV and 40 mA, step width of 0.013°, count time of 18.87 sec/step) (Doktorovova et al. 2011).

Scanning electron microscopy (SEM)

Morphological examination of empty nanoparticles and their complexes with pDNA, SEM was performed at Central Research Laboratory in Izmir Katip Celebi University, Turkey. After preparing the nanoparticle samples with or without pDNA, the samples were diluted at least 7-fold in upH_2O. Then, each sample (5 μL) was dried on a glass coverslip for 24 h in a desiccator at room temperature. Before imaging, the samples were sputter coated with ~8 nm conductive layer of gold under high vacuum using Quorum Q150R ES (Quorum Technologies, UK). The complexes were examined using Carl ZEISS Sigma 300 VP SEM (ZEISS Group, Germany) operating at 2.00 kV via InLens secondary electron detector.

Cell culture and XTT cell viability assay

L-929 mouse fibroblast cell line (CCL-1, ATCC) was a kind gift from Assoc. Prof. PhD Vildan Bozok-Cetintas from Department of Medical Biology, Faculty of Medicine, Ege University. L-929 cells were cultured in DMEM supplemented with 10% FBS (heat-inactivated at 56°C for 30 min), 1% P/S solution in the atmosphere humidified with 5% CO_2 at 37 °C.

To assess the cytotoxicity of the nanoparticles, we performed a spectrophotometric method based on the fact that metabolically active viable cells reduce the colorless XTT tetrazolium salt to an orange-colored compound of formazan. XTT is a water-soluble tetrazolium salt like WST and MTS, which was developed to eliminate the necessary solubilization step for MTT assay (Paull et al. 1988; Doktorovova et al. 2014). For cell viability assay, L929 cells were seeded into 96-well

plates at the density of $5x10^3$ cells/200 µL and incubated for 48 h. After the incubation period, the media were removed and 200 µL media including the formulations at different concentrations (0.5-10 mg/mL for cSLNs and 0.5-2.5 mg/mL for cNLCs) were added to the wells. While determining the concentration range of SLNs and NLCs, six points were chosen- by having at least one concentration higher and one concentration lower than the concentration where ~50% cell death occurred- to calculate the half-lethal concentration (LC_{50}) value more accurately. The applied concentrations were calculated according to all ingredients used to prepare formulation, except water. After 48 h treatment, the media were replaced with a mixture of fresh medium and XTT detection solution (100 µL: 50 µL) and incubated for an additional 4 h as per manufacturer's instructions (Biological Industries, Israel). At the end of the incubation period, absorbance was measured at 450 nm using Varioskan Flash multimode reader (Thermo Scientific, USA). Absorbance was also measured at 650 nm as a reference wavelength to eliminate non-specific readings. Each experiment included the background control (B, containing complete medium without cells). The net absorbance value (A_{450}-A_{650}-A_B) was graphed as percentage cell viability relative to the untreated group (UT) using GraphPad Prism 6.0 (GraphPad Software, Inc., USA).

The LC_{50} value of cSLNs and cNLCs was calculated by CompuSyn software using the concentration- percentage cell viability data (Chou & Martin 2005).

Statistical Analysis

Results were expressed as arithmetic mean ± standard deviation (mean ± SD) of at least three measurements unless otherwise specified. Statistical analysis was performed using GraphPad Prism 6 software (GraphPad Software Inc., USA). P-value < 0.05 was considered statistically significant. Ordinary two-way ANOVA with a Bonferroni's post hoc multiple comparisons test was performed for cytotoxicity (**Figure 4**) and stability

(**Figure 5**) experiments. An unpaired, two-tailed *t-test* was used for the comparison of each formulation relative to UT control (**Supplementary Figure 1**).

Results and Discussion

Development of NLCs from SLN

As a model nanoparticle system to develop NLCs, an SLN formulation with desirable characteristics (small particle size and distribution, long stability, *etc.*) was needed. In a previous study, we successfully prepared two different SLNs containing Precirol ATO 5 (P) or Compritol 888 ATO (C) as a solid lipid by the hot microemulsion stepwise method and investigated their physicochemical characteristics and cytotoxicity. It was determined that SLN with P had a smaller particle size than SLN with C (22 ± 0.4 nm *vs.* 33 ± 0.5 nm), and was more cytotoxic to L-929 mouse fibroblast cells (IC_{50}= 475 µg/mL *vs.* 1440 µg/mL) (Kotmakçı et al. 2016). Thus, in this study, we prepared a new SLN formulation (SLN3) containing a blend of P & C solid lipids at 1:1 (w/w) ratio by modifying this microemulsion stepwise method to create a formulation possessing both small particle size and less toxicity. The SLNs containing only P or C (designated SLN1 and SLN2, respectively) were also prepared by this modified method and their stability was compared with each other (**Figure 1**). Even with close similarity in physicochemical characteristics of those SLNs in terms of zeta potential, particle size and PDI after preparation (**Figure 1-A**), only SLN1 formed aggregates after 2.5 months of storage at room temperature (**Figure 1-B**). Both SLN3 and SLN2 did not form aggregates and showed similar stability during 4 months of storage (**Figure 1-A**). It was postulated that blending solid lipids may produce a less ordered crystalline matrix and lead to a more stable system in the long-term. Therefore, SLN3 formulation containing P and C at 1:1 (w/w) ratio was selected to proceed for preparation of all other (c)SLN

and (c)NLC formulations.

Here, we proposed a new approach to derive NLCs from an SLN formulation by considering the HLB values of solid lipids (SLs) and liquid lipids (LLs). Six different NLC formulations (NLC1-6) were derived from SLN3 formulation using **Equation 1**. As shown in **Table 3**, all NLC formulations- except NLC5- had a close similarity to SLN3 formulation in terms of particle size (25-27 nm), polydispersity (PDI< 0.2), and zeta potential (between -10 mV and -5 mV). Incorporating LWL to the structure of NLCs caused an increase in the PDI values of all formulations. This increase was negligible when LWL was combined with L90 (NLC1 and NLC3). However, when LWL was combined with PGMC (NLC5), this increase in PDI was more obvious.

To explain the high PDI and particle size of NLC5, differences in the structure and functionality of the liquid lipids should be considered. LPG, L90, and PGMC are composed of propylene glycol esters, and they were previously reported to function as co-surfactants (Barakat 2010; Lee et al. 2014; Salimi et al. 2014). On the other hand, LWL is composed of highly lipophilic triglycerides which do not have a co-surfactant function. Also, it was previously demonstrated that using triglycerides instead of dipropylene glycol esters in the structure of NLCs increased particle size and polydispersity (Date & Nagarsenker 2019). Keeping these in mind, NLC6 had small particle size and low PDI value due to the co-surfactant effect of both LPG and PGMC. However, in the case of NLC5, there was only low concentration of PGMC to function as a co-surfactant. Therefore, this may be the reason for the increase in PDI and particle size of NLC5. Besides, NLC1 and NLC3 included higher amounts of L90 when compared to PGMC amount in NLC5. Thus, the total co-surfactant concentration in these systems was higher than NLC5 (**Table 2**), and there was not a notable change in their characteristic.

All in all, it was concluded that 5 out of 6 NLC formulations were successfully developed from SLN3 in terms of physicochemical characteristics by equalizing the total HLB values of solid lipids to liquid lipids without changing the total lipid weight.

Development of cSLNs

Positively charged nanoparticles have many advantages such as easily interacting with the negatively charged cell membrane and being used as a carrier system for nucleic acids (pDNA, siRNA, miRNA, *etc*.). In many studies, cationic lipid nanoparticles are developed for drug and gene delivery purposes. One of the major advantages of cationic lipid-based nanoparticles over other gene delivery systems is the opportunity for the co-delivery of the nucleic acids and the lipophilic drugs.

Cationic lipids are included in the composition of the formulations for providing a positive charge to the nanoparticles. Generally, double-tailed cationic lipids (EQ1, DDAB, DOTAP, DOTMA, *etc*.) are determined as less toxic and more efficient for transfection than the single-tailed and three-tailed ones (Tabatt et al. 2004; Zhi et al. 2010). Therefore, we chose EQ1 and DDAB cationic lipids including double-tailed aliphatic chains for preparing cationic solid lipid nanoparticles (cSLNs).

cSLNs containing 0.5% (w/w) and 1% (w/w) cationic lipids were first prepared based on SLN3 formulation. The amount of the solid lipids excluded from the SLN3 formulation was equal to the amount of the cationic lipid added to the composition. Non-cationic forms of those cSLNs were also prepared for comparing the effects of the different solid lipid ratios (4% and 4.5%) and the cationic lipids on formulations.

The results obtained from particle size, PDI, and ZP measurements (**Table 4**) showed that SLN5 formulation containing 4% SL had a slightly smaller particle size and a lower particle size distribution than SLN4 and SLN3 formulations containing 4.5% SL and 5% SL, respectively. Although addition of cationic lipids (EQ1 or DDAB)

provided a positive surface charge to these SLNs, they caused an undesirable increase in PDI. This increase in PDI was higher in DDAB-cSLNs than EQ1-cSLNs at both cationic lipid concentrations (0.5% and 1%; w/w). Taking this into account and considering that DDAB was more toxic than EQ1 as demonstrated previously (Tabatt et al. 2004), we decided to continue with the formulations containing 4% SL and EQ1 as a cationic lipid for further studies.

For determining the optimum S/CoS and EQ1 concentrations, various cSLN formulations containing 4% SL and different concentrations of S/CoS (4%, 8%, 18%) and EQ1 (0.2%-0.5%) were prepared. As presented in **Figure 2**, the particle size of all EQ1-cSLN formulations were under 100 nm and there was a close similarity in the particle size between each S/CoS group. The zeta potential of EQ1-cSLNs was gradually decreased by increasing the S/CoS concentration and it was reduced to below +20 mV at the highest S/CoS concentration (18%). The ZP value of cSLN9 was also below +20 mV. Furthermore, ZP values of cSLNs containing EQ1 at 0.3%, 0.4% and 0.5% (w/w) ratios was similar when each S/CoS group was compared individually. It is known that cationic lipids/surfactants and their increased concentrations are associated with high toxicity (Xue et al. 2012; Bose et al. 2015). Therefore, we think that choosing the lowest concentration of cationic lipid may ensure a better cell compatibility. Moreover, it is well-known that an absolute zeta potential value above 30 mV is a predictor of good stability (Honary & Zahir 2013). Although cSLN10 containing 8% S/CoS had a +25 mV zeta potential, we also included it in further studies to compare with cSLN6 containing 4% S/CoS. Based on the above data, cSLN6 and cSLN10 formulations containing 0.3% EQ1 were selected as cSLN models for obtaining cNLCs.

Development of cNLCs from cSLNs

Eight different cNLCs were derived from cSLNs containing 0.3% EQ1 with 4% and 8% S/CoS, and the measurements of D, PDI, and ZP were performed (**Figure 3**). As a result of using LPG instead of LWL, there was a slight increase in particle size with cNLCs prepared at 3.5:1.5 SL:LL ratio. However, there was a slight decrease in size with cNLCs prepared at 3:2 SL:LL ratio. These differences in size were more obvious for cNLCs with 4% S/CoS than cNLCs with 8% S/CoS. Zeta potential values were approx. +30 mV for cNLCs with 4% S/CoS and approx. +20 mV for cNLCs with 8% S/CoS. Based on these results, it was observed that the D, PDI and ZP values of all cNLCs were similar to their model cSLNs [cSLN6 for cNLC(1-4); cSLN10 for cNLC(5-8)]. Thus, we concluded that all cNLCs were successfully prepared from their precursor cSLNs.

Determination of the cytotoxicity of cSLNs and cNLCs

L-929 mouse fibroblast cell line is commonly used to investigate the biocompatibility of the materials and cytotoxicity of the nanoparticles in the literature (ISO/EN10993-5 2009; Skladanowski et al. 2016; Minaeva et al. 2017). Before proceeding to further studies, a preliminary cytotoxicity test was performed with cNLCs containing 8% S/CoS in L-929 cells to choose the SL:LL ratio. Although all tested formulations had similar physicochemical characteristics, it was observed that higher LL concentration (3:2 SL:LL ratio) caused higher toxicity (**Supplementary Figure 1)**. Therefore, cNLCs with a low concentration of LL (3.5:1.5 SL:LL ratio) were selected for determining the LC_{50} value.

After selecting the cSLN and cNLC formulations, they were applied to L-929 cells to investigate the effect of S/CoS concentration and type of the liquid lipid on cytotoxicity and determine their LC_{50} values (**Figure 4**). As a result of partially

replacing SLs with the same amount of LLs, cNLCs showed higher cytotoxicity than cSLNs (LC_{50} values: cSLN6> cSLN10> cNLC5> cNLC6> cNLC1> cNLC2). Also, using LPG instead of LWL in the composition increased the cytotoxicity of cNLCs at both S/CoS concentrations, probably due to the higher toxic effect of LPG than LWL on this cell line. Using high surfactant levels did not cause a statistically significant change in the cytotoxicity of cSLNs, but it decreased the cytotoxicity of cNLCs. This decrease was statistically significant at 0.75-1.5 mg/mL concentrations for LWL-cNLCs and 0.5-1 mg/mL concentrations for LPG-cNLCs ($p<0.05$).

There are few studies directly comparing the cytotoxicity SLNs *vs.* NLCs (Ruktanonchai et al. 2009; Dong et al. 2009; Fang et al. 2011). Based on these cytotoxicity studies, it is hard to say the advantage of one system over another. We didn't come across any direct comparison cytotoxicity study of cSLNs *vs.* cNLCs; however, the addition of cationic lipids to the structure increases the cytotoxicity of nanoparticles. In this study, cSLNs were found less cytotoxic than cNLCs, however, the LC_{50} value of the developed formulations was well-above the previously developed cationic formulations (Doktorovova et al. 2014). Therefore, we concluded that all formulations were well-tolerated by L-929 cells.

Storage stability of cSLNs and cNLCs

Solid lipid nanoparticles and nanostructured lipid carriers are known as stable systems among all lipid-based formulations (Shidhaye et al. 2008). In the literature, it was demonstrated several times that NLCs are more stable than SLNs as lipophilic drug-carriers due to the contribution of liquid lipid(s) to the imperfect matrix structure (Das et al. 2012; Tosta et al. 2014; Kelidari et al. 2017). Thus, the determination of the storage stability is an important parameter for these carriers.

Here, we firstly investigated the effect of storage on particle size, PDI, and ZP of the selected cSLN and cNLCs. As shown in **Figure 5**, no significant changes in particle size and zeta potential of formulations were observed after 3-months ($p>0.05$). Therefore, it can be said that all formulations are stable after 3-months storage at room temperature. After 24-months, there was an insignificant increase in the particle size of formulations containing 8% S/CoS ($p>0.05$). This increase in particle size did not occur with the formulations containing 4% S/CoS, most likely due to their higher zeta potential (electric repulsion). All formulations showed a decrease in PDI values, but this change was statistically significant only for cNLC5. The decrease in ZP values was slighter with cNLCs than cSLNs. Based on the 24-months stability results, the formulations containing 4% S/CoS are more stable than those with 8% S/CoS in terms of particle size.

Among these formulations, time-dependent change in the crystalline structure of cSLN6 and cNLC1, which have the highest complexation capacity with pDNA (see next section), were further characterized by DSC and XRD (**Figure 6**). First, DSC analysis was performed to evaluate the melting and crystallinity profiles of solid materials in these formulations (**Figure 6-A**). The onset temperature, melting point, and enthalpy values are calculated from the thermograms of solid materials in powder form (bulk) and their physical mixtures prepared at the same ratio as in formulations (**Table 5**). The enthalpy of each physical mixture was lower than the total enthalpy of bulk materials. Thus, the required energy for phase transition (*i.e.* crystallinity) of solid materials is less when they are mixed (Vighi et al. 2007; Pathak & Nagarsenker 2009). Moreover, no melting peaks were detected with cSLN6 and cNLC1 formulations. This may indicate that the solid lipids are not in crystalline form in these formulations

(Kotmakçı et al. 2016). Furthermore, there was no apparent change in DSC thermograms of formulations after 24-months of storage at room temperature.

The time-dependent change in the crystallinity profile of formulations was also investigated by a wide-angle X-Ray scattering (WAXS) method (**Figure 6-B**). According to the XRD patterns of dispersions, the characteristic peaks of solid lipids Precirol and Compritol were observed at 2θ values (the degree at maximum intensity peak) between 19° and 22°, as previously demonstrated (Pathak & Nagarsenker 2009). There was no shift at 2θ values of these solid lipids, and their peak intensities were similar when XRD patterns of the formulations 'Day 0' and '24-months' were overlapped. Thus, there is no noticeable polymorphic transition of solid lipids included in the formulations. In accordance with DSC measurements, XRD results showed that cSLN6 and cNLC1 are stable in terms of crystallinity even after 24-months of storage at room temperature.

Nucleic acid binding capacity of cSLNs and cNLCs

For gene delivery purposes; non-viral delivery systems have many advantages like cost-effectiveness, ease of production and scalability compared to the viral vectors, which may cause severe side effects and immune responses (Yin et al. 2014). As a first step to investigate the suitability of the selected nanoparticles for use in gene delivery, we performed a nucleic acid binding assay. To our knowledge, this is the first study directly comparing the nucleic acid binding capacity of cSLNs *vs.* cNLCs.

First, we measured the pH of the selected cSLNs and cNLCs diluted in PBS or upH_2O; and then determined their complexation capacity with pDNA in these mediums. Both cSLNs and cNLCs displayed more acidic character in upH_2O than in PBS (**Table 6**). This can be explained by the buffer effect of PBS, which changed the pH of the formulations to its' pH value (~7.4). Based on the results from gel shift assay (**Figure 7-**

A1), the pDNA binding ability of all formulations diluted in upH_2O was higher than the ones diluted in PBS. The interaction between the negatively charged phosphate ions of PBS and the positively charged quaternary ammonium groups of EQ1 probably caused formulations' displaying more neutral surface charge in PBS than in water (Agirre et al. 2015; Di Ianni et al. 2017). Moreover, all formulations containing 4% S/CoS had better pDNA binding ability than those containing 8% S/CoS. Similarly, Kim et al. (2002) observed a decreased pDNA binding ability by increasing the surfactant ratio because of the steric hindrance effect of polyethylene glycol (PEG) chains involved in non-ionic surfactants. KRH40 involved in the S/CoS mixture of our formulations is also a non-ionic surfactant having PEG chains. Therefore, the high S/CoS (*i.e.* KRH40) ratio may have hindered the quaternary ammonium groups of EQ1 on the nanoparticles' surface, subsequently leading to a decrease in zeta potential and eventually low pDNA binding ability. However, the pDNA binding capacity of cSLNs was lower than cNLCs, although the zeta potential of all cSLN and cNLC formulations were similar to each other. It may be explained by the higher matrix mobility of cNLCs than cSLNs due to the addition of thermodynamically unstable oils in their structure (Khalil et al. 2014; Shah et al. 2015). More mobile matrix, hence higher flexibility of the surface, may provide adaptation to a more suitable shape for binding pDNA. The slightly more acidic nature of cNLCs (**Table 6**) may be another reason for the higher pDNA binding capacity over cSLNs, as the positive charge of nanoparticles is preserved by the effect of protonation in a relatively more acidic environment (Blane & Fanucchi 2015). Furthermore, the lowest pDNA binding ability occurred with cSLN10 as compared to others. cNLC1, which bound pDNA at N/P ratio of 15 even when diluted in PBS, showed the best complexation ability with pDNA.

Among the prepared formulations, one SLN (cSLN6) and one NLC (cNLC1) showing the best complexation with pDNA were selected for further investigation of their siRNA binding capacity. Unexpectedly, none of these formulations completely bound siRNA despite the high N/P ratios (**Figure 7-A2** and **Figure 7-A3**). cNLC1 bound more siRNA at higher N/P ratio, however, this concentration is too high for applications in cell culture experiments. Similar results were reported by other researchers investigating different delivery systems (Kwok et al. 2016).

This difference between pDNA and siRNA binding capacity of nanoparticles may result from the smaller and more rigid structure of siRNA than pDNA. For measuring the helix rigidity, the persistence length is defined as the minimum length for a double-stranded nucleic acid to be able to fold (Hagerman 2002; Kwok et al. 2016). siRNA (~6 nm length) displays a rigid structure due to its ~70 nm persistence length, where pDNA is more flexible than siRNA by usually adapting a much larger size than its persistence length (~50 nm) (Jiang et al. 2013; Kwok et al. 2016). Thus, siRNA may not adapt into the suitable shapes for binding to cationic nanoparticles due to its inflexible nature. Also, the shorter length of siRNA (siEphA2: 21 base pairs) decreases the chance of electrostatic interactions with cationic nanoparticles when compared with the larger pDNA (pSIH1-puro-control shRNA: ~7200 base pairs) (Bishop et al. 2015; Kwok et al. 2016). Consequently, we concluded that the cSLNs and cNLCs developed in this study are potentially useful formulations for carrying pDNA, but not siRNA.

After selecting an optimum N/P ratio among the investigated N/P ratios for each formulation, the physicochemical characterization of all pDNA:nanoparticle complexes were performed using Zetasizer NanoZS instrument. As expected, there was an increase in particle size and a decrease in ZP of all formulations after complexing with pDNA (**Figure 7-B**). PDI of all pDNA:nanoparticle complexes was under 0.3, which presents a

narrow distribution. Moreover, the morphology analysis was conducted with cSLN6 and cNLC1 formulations showing the highest pDNA binding ability in each group. Based on the scanning electron microscopy images (**Figure 7-C**), both empty nanoparticles and their pDNA complexes had spherical/oval shape.

Conclusion

In this study, we observed that equalizing the HLB values of LLs to SLs is useful to develop (c)NLCs with a similar D, PDI, and ZP values to their precursor (c)SLNs. Besides HLB values, the structure (aliphatic chain number) and functionality (co-surfactant effect) of LLs should also be considered when applying this approach. Although future studies conducted with different solid and liquid lipids are needed to support this approach, we conclude that it has the potential to shorten the period for formulation optimization. Within the scope of this research, the comparison of cSLN and cNLC was limited with the stability, cytotoxicity, and nucleic acid binding ability assays. Further studies- including transfection experiments- are required to better compare these carriers as gene delivery systems in a particular disease.

Supplemental Material

Supplementary data is available.

Acknowledgements

This work was supported by The Scientific and Technological Research Council of Turkey (TUBITAK) under Grant number: 217S212. Special thanks to Assoc. Prof. MB PhD Stephen P. Finn from Department of Histopathology and Morbid Anatomy, Trinity College Dublin for editing and proofreading this article. We are grateful to Department of Pharmaceutical Technology, Faculty of Pharmacy, Ege University for providing access to Zetasizer NanoZS and also to Pharmaceutical Sciences Research Center (FABAL), Faculty of Pharmacy, Ege University for supplying Varioskan Flash multimode reader. PhD Nusret Kaya

from Central Research Laboratory in Izmir Katip Celebi University and MSc Nurdan Akakce from EGE-MATAL are greatly appreciated for their help with XRD and DSC analyses, respectively.

Disclosure statement

The authors report no conflict of interest.

References

Agirre M, Zarate J, Puras G, Ojeda E, Pedraz JL. 2015. Improving transfection efficiency of ultrapure oligochitosan/DNA polyplexes by medium acidification. Drug Deliv. 22:100–110.

Anselmo AC, Mitragotri S. 2016. Nanoparticles in the clinic. Bioeng Transl Med. 1:10–29.

Bahari LAS, Hamishehkar H. 2016. The impact of variables on particle size of solid lipid nanoparticles and nanostructured lipid carriers; A comparative literature review. Adv Pharm Bull. 6:143–151.

Balguri SP, Adelli GR, Majumdar S. 2016. Topical ophthalmic lipid nanoparticle formulations (SLN, NLC) of indomethacin for delivery to the posterior segment ocular tissues. Eur J Pharm Biopharm. 109:224–235.

Barakat NS. 2010. Self-emulsifying system for improving drug dissolution and bioavailability: In vitro/in vivo evaluation. Drug Dev Res. 71:149–158.

Barichello JM, Ishida T, Kiwada H. 2010. Complexation of siRNA and pDNA with Cationic Liposomes: The Important Aspects in Lipoplex Preparation. In: Weissig V, editor. Liposomes, Methods Mol Biol. Vol. 605; p. 461–472.

Bishop CJ, Kozielski KL, Green JJ. 2015. Exploring the role of polymer structure on intracellular nucleic acid delivery via polymeric nanoparticles. J Control Release. 219:488–499.

Blane A, Fanucchi S. 2015. Effect of pH on the Structure and DNA Binding of the FOXP2 Forkhead Domain. Biochemistry. 54:4001–4007.

Bose RJC, Arai Y, Ahn JC, Park H, Lee SH. 2015. Influence of cationic lipid concentration on properties of lipid–polymer hybrid nanospheres for gene delivery. Int J Nanomedicine. 10:5367–5382.

Chou T-C, Martin N. 2005. CompuSyn for Drug Combinations: PC Software and User's Guide: A Computer Program for Quantitation of Synergism and Antagonism in Drug Combinations, and the Determination of IC50 and ED50 and LD50 Values. [New Jersey (US)]: ComboSyn Inc; [accessed 2019 Oct 10]. http://www.combosyn.com/index.html.

Das S, Chaudhury A. 2011. Recent Advances in Lipid Nanoparticle Formulations with Solid Matrix for Oral Drug Delivery. AAPS PharmSciTech. 12:62–76.

Das S, Ng WK, Tan RBH. 2012. Are nanostructured lipid carriers (NLCs) better than solid lipid nanoparticles (SLNs): Development, characterizations and comparative evaluations of clotrimazole-loaded SLNs and NLCs? Eur J Pharm Sci. 47:139–151.

Date AA, Nagarsenker MS. 2019. Single-step and low-energy method to prepare solid lipid nanoparticles and nanostructured lipid carriers using biocompatible solvents. Eur J Pharm Res. 1:12–19.

Doktorovova S, Shegokar R, Rakovsky E, Gonzalez-Mira E, Lopes CM, Silva AM, Martins-Lopes P, Muller RH, Souto EB. 2011. Cationic solid lipid nanoparticles (cSLN): Structure, stability and DNA binding capacity correlation studies. Int J Pharm. 420:341–349.

Doktorovova S, Souto EB, Silva AM. 2014. Nanotoxicology applied to solid lipid nanoparticles and nanostructured lipid carriers - A systematic review of in vitro data. Eur J Pharm Biopharm. 87:1–18.

Dong X, Mattingly CA, Tseng M, Cho M, Adams VR, Mumper RJ. 2009. Development of new lipid-based paclitaxel nanoparticles using sequential simplex optimization. Eur J Pharm Biopharm. 72:9–17.

Fang Y-P, Lin Y-K, Su Y-H, Fang J-Y. 2011. Tryptanthrin-Loaded Nanoparticles for Delivery into Cultured Human Breast Cancer Cells, MCF7: the Effects of Solid Lipid/Liquid Lipid Ratios in the Inner Core. Chem Pharm Bull. 59:266–271.

Gasco MR, inventor. 1993 Oct 5. Method for producing solid lipid microspheres having a narrow size distribution. US5250236A. https://patents.google.com/patent/US5250236A/en

Gupta B, Yong CS, Kim JO. 2017. Solid matrix-based lipid nanoplatforms as carriers for combinational therapeutics in cancer. J Pharm Investig. 47:461–473.

H. Muller R, Shegokar R, M. Keck C. 2011. 20 Years of Lipid Nanoparticles (SLN & NLC): Present State of Development & Industrial Applications. Curr Drug Discov Technol. 8:207–227.

Hagerman PJ. 2002. Flexibility of Rna. Annu Rev Biophys Biomol Struct. 26:139–156.

Honary S, Zahir F. 2013. Effect of zeta potential on the properties of nano-drug delivery systems - A review (Part 2). Trop J Pharm Res. 12:265–273.

Hoshyar N, Gray S, Han H, Bao G. 2016. The effect of nanoparticle size on in vivo pharmacokinetics and cellular interaction. Nanomedicine. 11:673–692.

Huang S, Sinicrope FA. 2010. Sorafenib Inhibits STAT3 Activation to Enhance TRAIL-Mediated Apoptosis in Human Pancreatic Cancer Cells. Mol Cancer Ther. 9:742–750.

Di Ianni ME, Islan GA, Chain CY, Castro GR, Talevi A, Vela ME. 2017. Interaction of Solid Lipid Nanoparticles and Specific Proteins of the Corona Studied by Surface Plasmon Resonance. J Nanomater. 2017.

[ISO/EN10993-5] International Organization for Standardization 10993-5 Biological evaluation of medical devices - Part 5: Tests for in vitro cytotoxicity methods. 3 Ed. 2009.

Jiang S, Eltoukhy AA, Love KT, Langer R, Anderson DG. 2013. Lipidoid-coated iron oxide nanoparticles for efficient DNA and siRNA delivery. Nano Lett. 13:1059–1064.

Kelidari HR, Saeedi M, Akbari J, Morteza-semnani K, Valizadeh H, Maniruzzaman M, Farmoudeh A, Nokhodchi A. 2017. Development and Optimisation of Spironolactone Nanoparticles for Enhanced Dissolution Rates and Stability. AAPS PharmSciTech. 18:1469–1474.

Khalil RM, Abd-Elbary A, Kassem MA, Ghorab MM, Basha M. 2014. Nanostructured lipid carriers (NLCs) versus solid lipid nanoparticles (SLNs) for topical delivery of meloxicam. Pharm Dev Technol. 19:304–314.

Khosa A, Reddi S, Saha RN. 2018. Nanostructured lipid carriers for site-specific drug delivery. Biomed Pharmacother. 103:598–613.

Kim TW, Kim YJ, Chung H, Kwon IC, Sung HC, Jeong SY. 2002. The role of non-ionic surfactants on cationic lipid mediated gene transfer. J Control Release. 82:455–465.

Kotmakçı M, Akbaba H, Erel G, Ertan G, Kantarcı G. 2016. Improved Method for Solid Lipid Nanoparticle Preparation Based on Hot Microemulsions: Preparation,

Characterization, Cytotoxicity, and Hemocompatibility Evaluation. AAPS PharmSciTech. 18:1355-1365

Kovacevic A, Savic S, Vuleta G, Müller RH, Keck CM. 2011. Polyhydroxy surfactants for the formulation of lipid nanoparticles (SLN and NLC): Effects on size, physical stability and particle matrix structure. Int J Pharm. 406:163–172.

Kwok A, McCarthy D, Hart SL, Tagalakis AD. 2016. Systematic Comparisons of Formulations of Linear Oligolysine Peptides with siRNA and Plasmid DNA. Chem Biol Drug Des. 87:747–763.

Lee DW, Marasini N, Poudel BK, Kim JH, Cho HJ, Moon BK, Choi HG, Yong CS, Kim JO. 2014. Application of Box-Behnken design in the preparation and optimization of fenofibrate-loaded self-microemulsifying drug delivery system (SMEDDS). J Microencapsul. 31:31–40.

Lombardi Borgia S, Regehly M, Sivaramakrishnan R, Mehnert W, Korting HC, Danker K, Röder B, Kramer KD, Schäfer-Korting M. 2005. Lipid nanoparticles for skin penetration enhancement - Correlation to drug localization within the particle matrix as determined by fluorescence and parelectric spectroscopy. J Control Release. 110:151–163.

Lundy DJ, Chen KH, Toh EKW, Hsieh PCH. 2016. Distribution of systemically administered nanoparticles reveals a size-dependent effect immediately following cardiac ischaemia-reperfusion injury. Sci Rep. 6:1–10.

Mehnert W, Mader K. 2002. Solid lipid nanoparticles Production, characterization and applications. Adv Drug Deliv Rev. 47:165–196.

Minaeva O V, Brodovskaya EP, Pyataev MA, Gerasimov M V, Zharkov MN, Yurlov IA, Kulikov OA, Kotlyarov AA, Balykova LA, Kokorev A V, et al. 2017. Comparative study of cytotoxicity of ferromagnetic nanoparticles and magnetitecontaining polyelectrolyte microcapsules. J Phys Conf Ser. 784:012038.

Müller RH, Mäder K, Gohla S. 2000. Solid lipid nanoparticles (SLN) for controlled drug delivery – a review of the state of the art. Eur J Pharm Biopharm. 50:161–177.

Naseri N, Valizadeh H, Zakeri-Milani P. 2015. Solid Lipid Nanoparticles and Nanostructured Lipid Carriers: Structure, Preparation and Application. Adv Pharm Bull. 5:305–13.

Park K. 2014. Controlled drug delivery systems: Past forward and future back. J Control Release. 190:3–8.

Pathak P, Nagarsenker M. 2009. Formulation and evaluation of lidocaine lipid nanosystems for dermal delivery. AAPS PharmSciTech. 10:985–992.

Paull KD, Shoemaker RH, Boyd MR, Parsons JL, Risbood PA, Barbera WA, Sharma MN, Baker DC, Hand E, Scudiero DA, et al. 1988. J. Heterocyclic Chem. 25: 911–914.

Ruktanonchai U, Bejrapha P, Sakulkhu U, Opanasopit P, Bunyapraphatsara N, Junyaprasert V, Puttipipatkhachorn S. 2009. Physicochemical Characteristics, Cytotoxicity, and Antioxidant Activity of Three Lipid Nanoparticulate Formulations of Alpha-lipoic Acid. AAPS PharmSciTech. 10:227–234.

Salimi A, Sharif Makhmal Zadeh B, Hemati AA, Akbari Birgani S. 2014. Design and evaluation of self-emulsifying drug delivery system (SEDDS) Of carvedilol to improve the oral absorption. Jundishapur J Nat Pharm Prod. 9.

Sánchez-López E, Espina M, Doktorovova S, Souto EB, García ML. 2017. Lipid nanoparticles (SLN, NLC): Overcoming the anatomical and physiological barriers of the eye – Part II - Ocular drug-loaded lipid nanoparticles. Eur J Pharm Biopharm. 110:58–69.

Shah R, Eldridge D, Palombo E, Harding I. 2015. Lipid Nanoparticles: Production, Characterization and Stability. Cham: Springer. (SpringerBriefs in Pharmaceutical Science & Drug Development; p. 1–9).

Shidhaye S, Vaidya R, Sutar S, Patwardhan A, Kadam V. 2008. Solid Lipid Nanoparticles and Nanostructured Lipid Carriers – Innovative Generations of Solid Lipid Carriers. Curr Drug Deliv. 5:324–331.

Skladanowski M, Golinska P, Rudnicka K, Dahm H, Rai M. 2016. Evaluation of cytotoxicity, immune compatibility and antibacterial activity of biogenic silver nanoparticles. Med Microbiol Immunol. 205:603–613.

Song A, Zhang X, Li Y, Mao X, Han F. 2016. Effect of liquid-to-solid lipid ratio on characterizations of flurbiprofen-loaded solid lipid nanoparticles (SLNs) and nanostructured lipid carriers (NLCs) for transdermal administration. Drug Dev Ind Pharm. 42:1308–1314.

Souto EB, Wissing SA, Barbosa CM, Müller RH. 2004a. Development of a controlled release formulation based on SLN and NLC for topical clotrimazole delivery. Int J Pharm. 278:71–77.

Souto EB, Wissing SA, Barbosa CM, Müller RH. 2004b. Evaluation of the physical stability of SLN and NLC before and after incorporation into hydrogel formulations. Eur J Pharm Biopharm. 58:83–90.

Tabatt K, Sameti M, Olbrich C, Müller RH, Lehr CM. 2004. Effect of cationic lipid and matrix lipid composition on solid lipid nanoparticle-mediated gene transfer. Eur J Pharm Biopharm. 57:155–162.

Teixeira MC, Carbone C, Souto EB. 2017. Beyond liposomes: Recent advances on lipid based nanostructures for poorly soluble/poorly permeable drug delivery. Prog Lipid Res. 68:1–11.

Tosta FV, Andrade LM, Mendes LP, Anjos JL V., Alonso A, Marreto RN, Lima EM, Taveira SF. 2014. Paclitaxel-loaded lipid nanoparticles for topical application: the influence of oil content on lipid dynamic behavior, stability, and drug skin penetration. J Nanoparticle Res. 16:1–12.

Vighi E, Ruozi B, Montanari M, Battini R, Leo E. 2007. Re-dispersible cationic solid lipid nanoparticles (SLNs) freeze-dried without cryoprotectors: Characterization and ability to bind the pEGFP-plasmid. Eur J Pharm Biopharm. 67:320–328.

Xue Y, Zhang S, Tang M, Zhang T, Wang Y, Hieda Y, Takeshita H. 2012. Comparative study on toxic effects induced by oral or intravascular administration of commonly used disinfectants and surfactants in rats. J Appl Toxicol. 32:480–487.

Yin H, Kanasty RL, Eltoukhy AA, Vegas AJ, Dorkin JR, Anderson DG. 2014. Non-viral vectors for gene-based therapy. Nat Rev Genet. 15:541–555.

Yu YH, Kim E, Park DE, Shim G, Lee S, Kim YB, Kim CW, Oh YK. 2012. Cationic solid lipid nanoparticles for co-delivery of paclitaxel and siRNA. Eur J Pharm Biopharm. 80:268–273.

Zhi D, Zhang S, Wang B, Zhao Y, Yang B, Yu S. 2010. Transfection efficiency of cationic lipids with different hydrophobic domains in gene delivery. Bioconjug Chem. 21:563–577.

Figure Captions with Footnotes

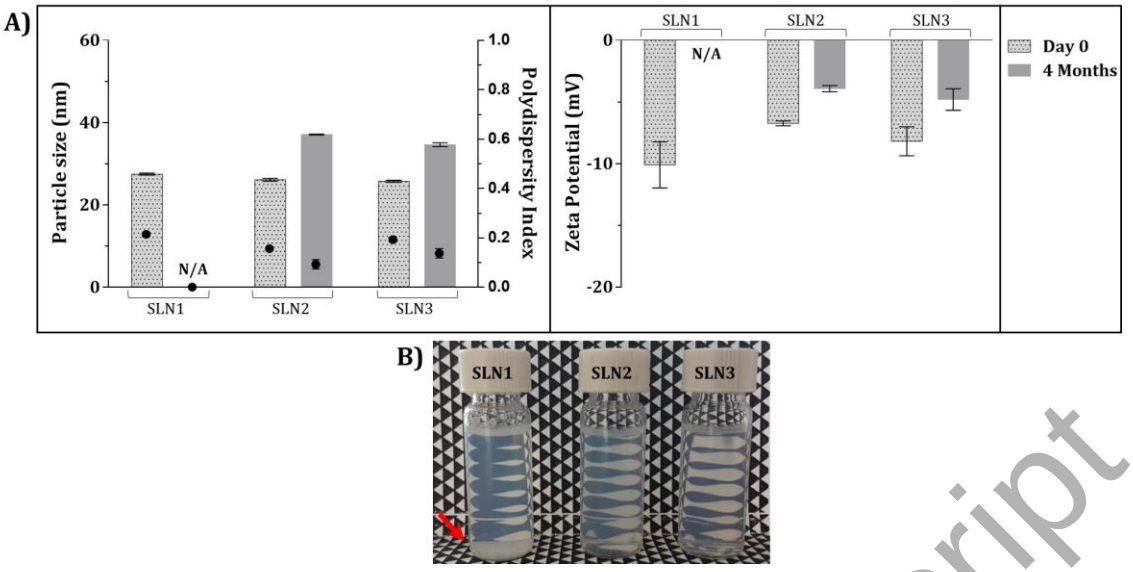

Figure 1. Long-term stability of SLNs containing Precirol ATO 5 and/or Compritol C888 ATO as solid lipid(s). The graphs showing the changes in particle size (D), polydispersity index (PDI) and zeta potential (ZP) after 4-months of storage at room temperature (**A**). Images of SLN vials were captured 2.5 months after preparation (**B**).

N/A: Not available. For the compositions of SLN formulations see **Table 1**. The red arrow shows the aggregate. Bars represent the D or ZP; dots represent PDI. The results are expressed as mean ± SD of three measurements.

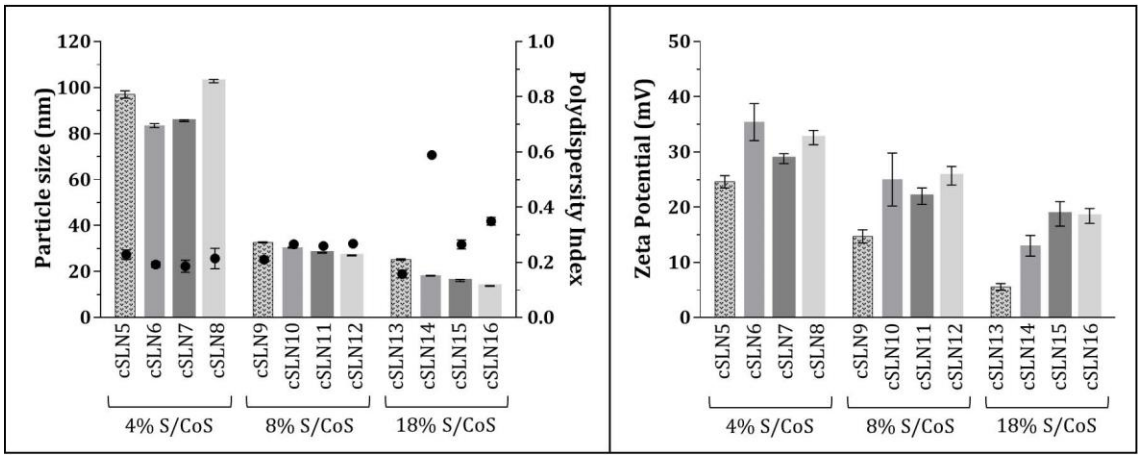

Figure 2. Physicochemical properties of cationic solid lipid nanoparticles prepared with different concentrations of S/CoS (4%, 8%, 18%) and EQ1 (0.2%-0.5%).

For the compositions of cSLN formulations see **Table 1**. Bars represent the particle size or zeta potential; dots represent polydispersity index. The results are expressed as mean ± SD of three measurements.

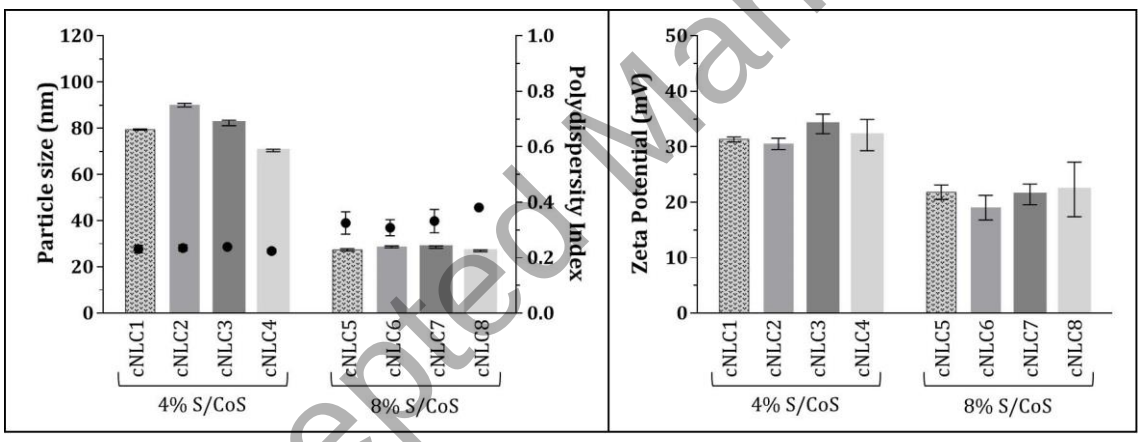

Figure 3. Physicochemical properties of cationic nanostructured lipid carriers containing 0.3% EQ1 with different concentrations of S/CoS.

For the compositions of cNLC formulations see **Table 2**. Bars represent the particle size or zeta potential; dots represent polydispersity index. The results are expressed as mean ± SD of three measurements.

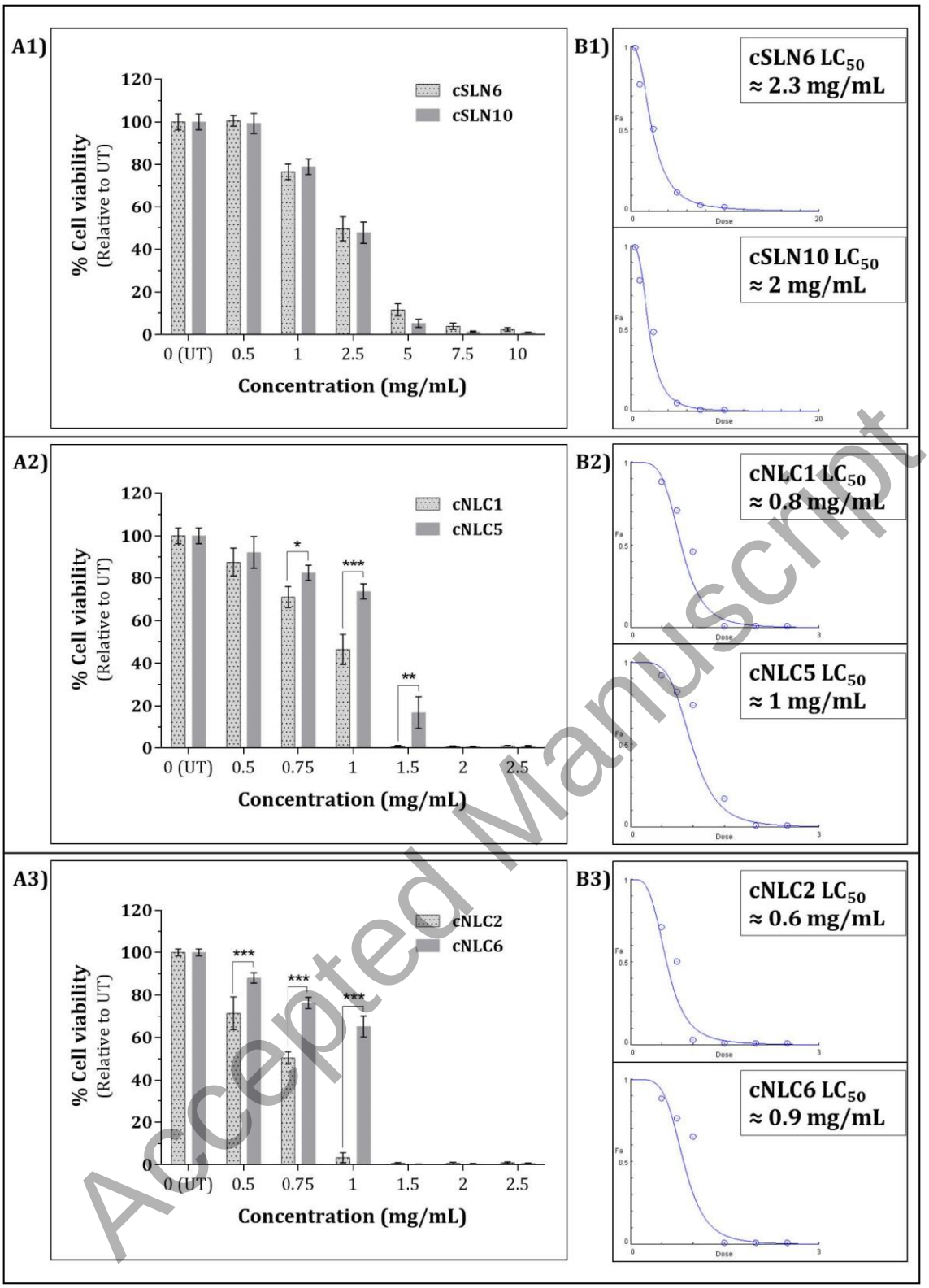

Figure 4. The effect of the selected cSLNs and cNLCs on cell viability in L-929 mouse fibroblast cells (48 h) (**A**) and the dose-response curves used for calculating LC_{50} value (**B**).

The graph and curves are regarding cSLNs (**A1** & **B1)**, LWL-cNLCs (**A2** & **B2**) and LPG-cNLCs (**A3** & **B3**). For the compositions of cSLNs see **Table 1** and for cNLCs see **Table 2**. The concentration of the formulations was calculated according to all ingredients (except water) used to prepare formulation. The results are graphed as mean ± SD (n=3). Asterisks represent significant difference between 4% and 8% S/CoS formulations at each concentration (*p<0.05, **p<0.01, ***p<0.001, ordinary two-way ANOVA with a Bonferroni's post hoc test).

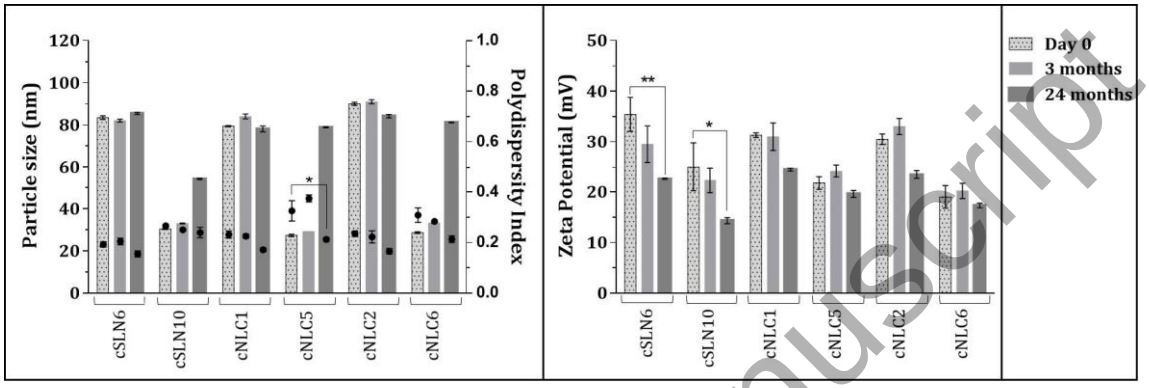

Figure 5. Storage stability of the selected cSLN and cNLC formulations.

The graphs are showing the changes in particle size (D) and polydispersity index (PDI) and zeta potential (ZP) after 3-months and 24-months storage at room temperature. For the compositions of cSLNs see **Table 1** and for cNLCs see **Table 2**. Bars represent the D or ZP; dots represent PDI. The results are expressed as mean ± SD of three measurements. Asterisks represent significant difference at each time point relative to 'day 0' (*p<0.05, **p<0.01, ordinary two-way ANOVA with a Bonferroni's post hoc test).

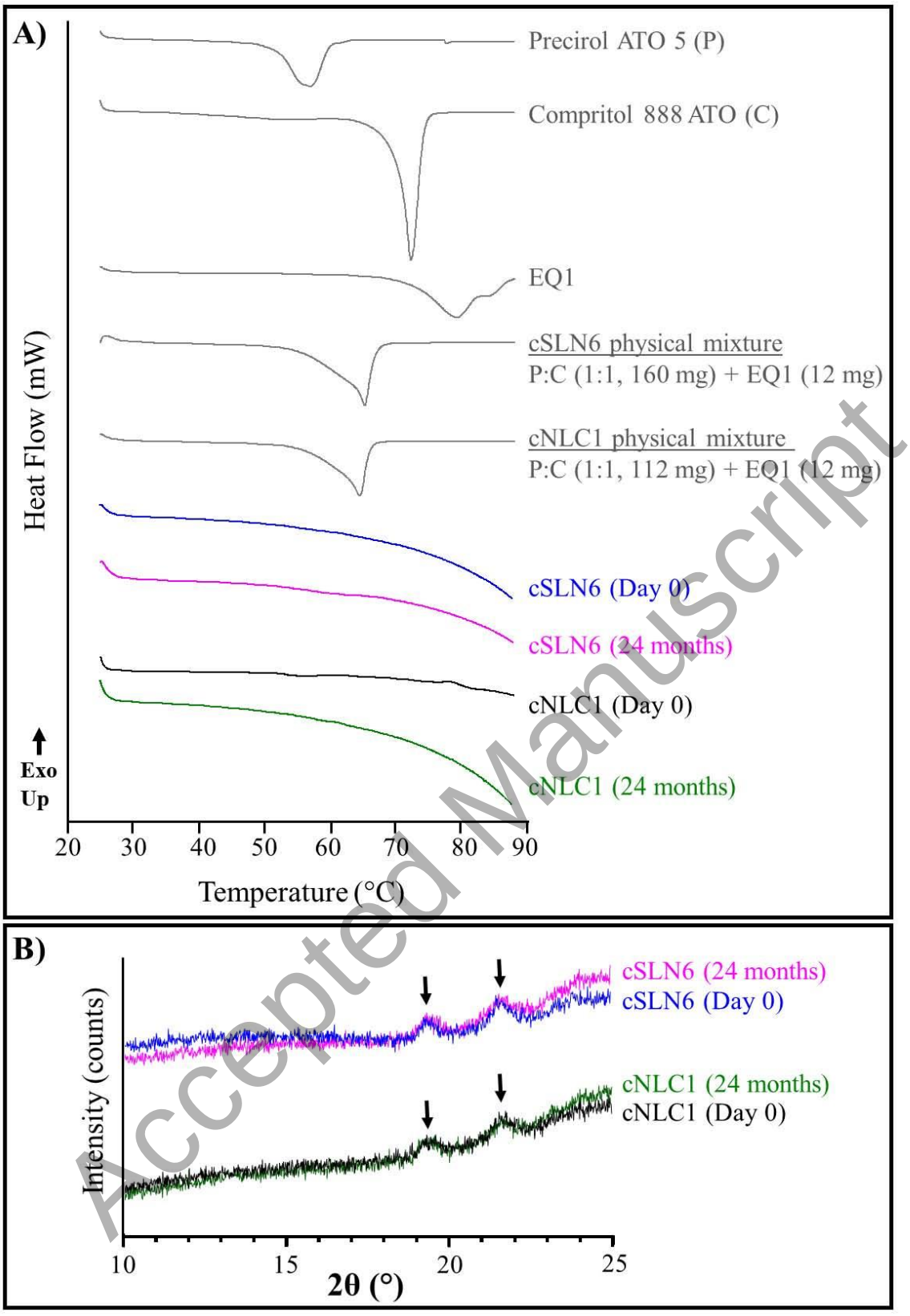

Figure 6. The change in DSC thermograms (**A**) and XRD patterns (**B**) of cSLN6 and cNLC1 formulations after 24-months storage at room temperature.

For the composition of cSLN6 see **Table 1** and for cNLC1 see **Table 2**.

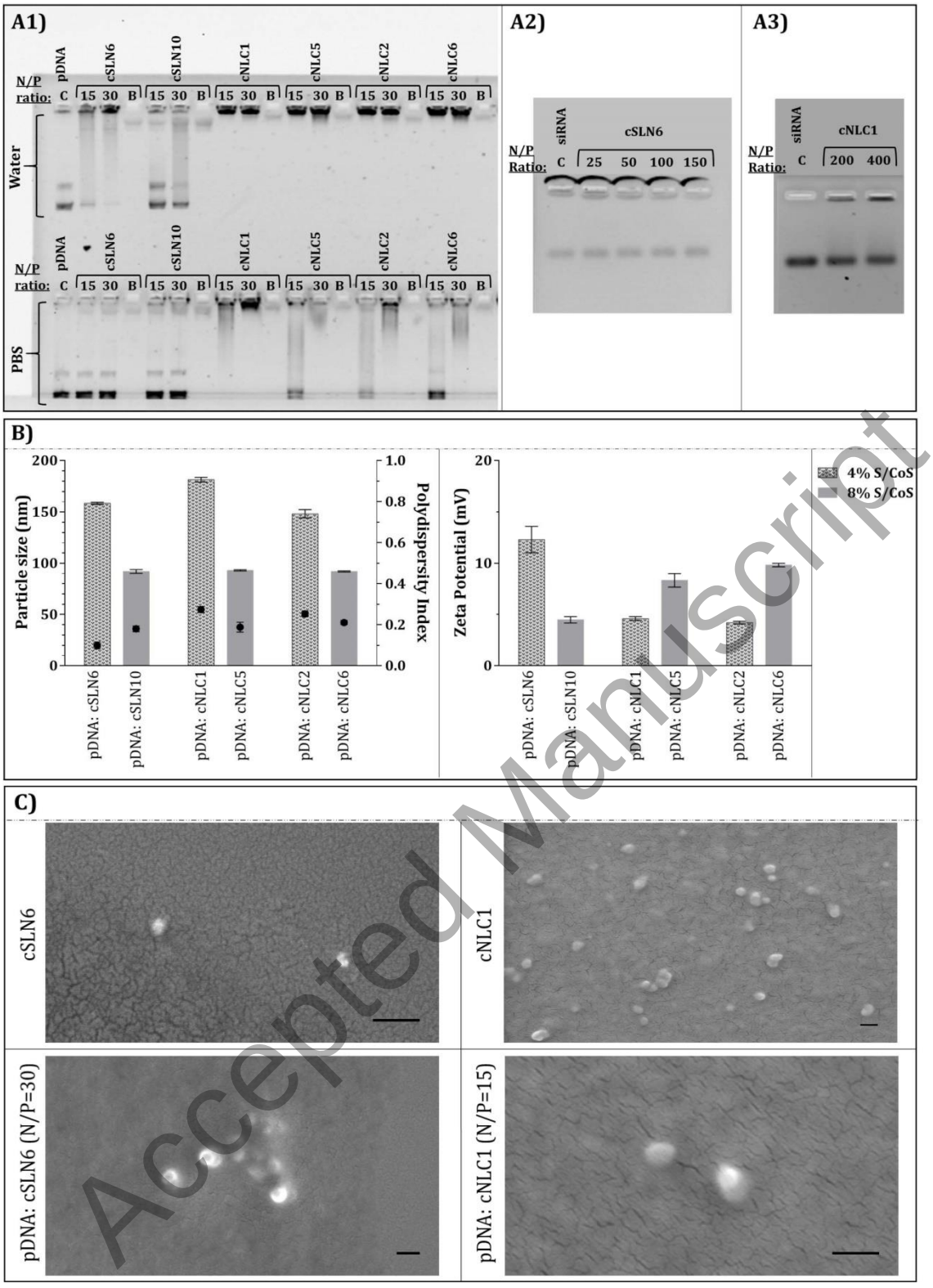

Figure 7. The pDNA binding abilities of the selected cSLNs and cNLCs diluted in upH_2O or PBS (**A1**), and the siRNA binding abilities of cSLN6 (**A2**) and cNLC1 (**A3**) diluted in upH_2O. Physicochemical properties of the pDNA:nanoparticle complexes at

N/P ratios of 30 and 15 for cSLNs and cNLCs, respectively (**B**). The scanning electron microscopy images of cSLN6 and cNLC1 with/ without pDNA (**C**).

C: Naked pDNA/siRNA. **B:** Blank vehicle (empty nanoparticle). 100 ng pDNA or 67 ng siRNA (2.5 µM, 2 µL) was loaded to each well. Samples were loaded on to 0.8% agarose gel in 1X TAE buffer (100V, 20 min) for pDNA and 2% agarose gel in 0.5X TBE buffer (100V, 15 min) for siRNA.

Bars represent the particle size or zeta potential; dots represent polydispersity index. The results are expressed as mean ± SD of three measurements.

SEM was performed by using Carl ZEISS Sigma 300 VP, operated at a voltage of 2 kV via InLens secondary electron detector. Scale bars, 200 nm.

Table 1. Compositions of the developed SLNs and cSLNs.

Code	P (%)	C (%)	S/CoS (%)	E (%)	D (%)	upH$_2$O (%)
SLN1	5		18	-	-	77
SLN2	-	5	18	-	-	77
SLN3	2.5	2.5	18	-	-	77
SLN4	2.25	2.25	18	-	-	77.5
cSLN1	2.25	2.25	18	0.5	-	77
cSLN2	2.25	2.25	18	-	0.5	77
SLN5	2	2	18	-	-	78
cSLN3	2	2	18	1	-	77
cSLN4	2	2	18	-	1	77
cSLN5	2	2	4	0.2	-	91.8
cSLN6	**2**	**2**	**4**	**0.3**	**-**	**91.7**
cSLN7	2	2	4	0.4	-	91.6
cSLN8	2	2	4	0.5	-	91.5
cSLN9	2	2	8	0.2	-	87.8
cSLN10	**2**	**2**	**8**	**0.3**	**-**	**87.7**
cSLN11	2	2	8	0.4	-	87.6
cSLN12	2	2	8	0.5	-	87.5
cSLN13	2	2	18	0.2	-	77.8
cSLN14	2	2	18	0.3	-	77.7
cSLN15	2	2	18	0.4	-	77.6
cSLN16	2	2	18	0.5	-	77.5

All ratios were based on the weights of materials. Total weight of each formulation was 4 g. The formulations in bold were selected for cytotoxicity study and nucleic acid binding assays.

P: Precirol ATO 5; **C:** Compritol C888 ATO; **S/CoS:** The mixture of surfactants and co-surfactant (KRH40:S80:PG; 3:1:4 w/w); **KRH40:** Kolliphor RH 40; **S80:** Span 80; **PG:** Propylene glycol; **E:** EQ1; **D:** DDAB; **upH$_2$O:** Ultra-pure water.

Table 2. Compositions of the developed NLCs and cNLCs.

Code	Solid lipid mixture (%) [a]	Liquid lipids (%) [b]				S/CoS (%)	E (%)	upH$_2$O (%)
		PGMC	L90	LWL	LPG			
NLC1	3.5	-	0.75	0.75	-	18	-	77
NLC2	3.5	-	0.75	-	0.75	18	-	77
NLC3	3	-	1	1	-	18	-	77
NLC4	3	-	1	-	1	18	-	77
NLC5	3	0.4	-	1.6	-	18	-	77
NLC6	3	0.4	-	-	1.6	18	-	77
cNLC1	**2.8**	**-**	**0.6**	**0.6**	**-**	**4**	**0.3**	**91.7**
cNLC2	**2.8**	**-**	**0.6**	**-**	**0.6**	**4**	**0.3**	**91.7**
cNLC3	2.4	-	0.8	0.8	-	4	0.3	91.7
cNLC4	2.4	-	0.8	-	0.8	4	0.3	91.7
cNLC5	**2.8**	**-**	**0.6**	**0.6**	**-**	**8**	**0.3**	**87.7**
cNLC6	**2.8**	**-**	**0.6**	**-**	**0.6**	**8**	**0.3**	**87.7**
cNLC7	2.4	-	0.8	0.8	-	8	0.3	87.7
cNLC8	2.4	-	0.8	-	0.8	8	0.3	87.7

[a] All formulations were prepared with a mixture of P:C (1:1 w/w) solid lipids.

[b] 2.8%:1.2% (w/w) corresponds to 3.5:1.5 SL:LL ratio. 2.4%:1.6% (w/w) corresponds to 3:2 SL:LL ratio.

All ratios were based on the weights of materials. Total weight of each formulation was 4 g.

The formulations in bold were selected for cytotoxicity study and nucleic acid binding assays.

P: Precirol ATO 5 (HLB=2); **C:** Compritol C888 ATO (HLB=2); **LWL:** Labrafac lipophile WL 1349 (HLB=1), **LPG:** Labrafac PG (HLB=1), **L90:** Lauroglycol 90 (HLB=3), **PGMC:** Capryol PGMC (HLB=6). **S/CoS:** The mixture of surfactants and co-surfactant (KRH40:S80:PG; 3:1:4 w/w); **KRH40:** Kolliphor RH 40; **S80:** Span 80; **PG:** Propylene glycol; **E:** EQ1; **D:** DDAB; **upH$_2$O:** Ultra-pure water.

Table 3. Physicochemical properties of NLC formulations derived from SLN3 formulation [a].

Formulation Code [b]	D (nm)	PDI	ZP (mV)
NLC1	25.43 ± 0.57	0.129 ± 0.008	-6.88 ± 1.12
NLC2	25.64 ± 0.14	0.114 ± 0.030	-6.67 ± 0.58
NLC3	25.19 ± 0.18	0.104 ± 0.017	-6.18 ± 1.03
NLC4	24.66 ± 0.32	0.100 ± 0.018	-6.52 ± 1.93
NLC5	37.13 ± 0.47	0.380 ± 0.008	-8.68 ± 0.07
NLC6	26.60 ± 0.08	0.101 ± 0.030	-5.35 ± 0.85

[a] SLN3 formulation; D= 25.92 ± 0.11 nm; PDI= 0.185 ± 0.013; ZP= -9.63 ± 0.82 mV.

[b] For the compositions of NLC formulations see **Table 2**.

D: Particle size, PDI: Polydispersity index, ZP: Zeta potential. The results are expressed as mean ± SD of three measurements.

Table 4. Physicochemical properties of SLNs and cSLNs derived from SLN3 formulation [a].

Formulation Code [b]	D (nm)	PDI	ZP (mV)
SLN4	23.99 ± 0.44	0.164 ± 0.005	-7.37 ± 0.98
cSLN1	19.83 ± 0.15	0.353 ± 0.005	22.10 ±1.40
cSLN2	19.18 ± 0.23	0.475 ± 0.003	22.20 ± 1.18
SLN5	22.65 ± 0.34	0.138 ± 0.006	-6.00 ± 0.65
cSLN3	16.05 ± 0.22	0.427 ± 0.004	24.10 ± 1.52
cSLN4	34.15 ± 0.52	1.000 ± 0.000	29.60 ± 1.05

[a] For SLN3 formulation; D= 25.92 ± 0.11 nm; PDI= 0.185 ± 0.013; ZP= -9.63 ± 0.82 mV.

[b] For the compositions of SLN and cSLN formulations see **Table 1**.

D: Particle size, PDI: Polydispersity index, ZP: Zeta potential. The results are expressed as mean ± SD of three measurements.

Table 5. DSC parameters of solid materials.

Material	Onset (°C)	Melting point (°C)	Enthalpy (J/g)
Precirol ATO 5	52.04	57.16	109.8
Compritol 888 ATO	70.52	72.37	115.0
EQ1	72.39	79.38	92.28
Physical mixture of cSLN6	61.87	65.35	88.29
Physical mixture of cNLC1	60.71	64.58	91.32

Table 6. pH of the selected cSLNs and cNLCs diluted in upH_2O and PBS at 1/10 ratio.

Formulation Code [a]	pH in upH_2O	pH in PBS
cSLN6	5.01 ± 0.93	7.13 ± 0.09
cSLN10	4.56 ± 0.76	7.19 ± 0.08
cNLC1	4.29 ± 0.37	7.31 ± 0.07
cNLC5	4.20 ± 0.31	7.25 ± 0.09
cNLC2	4.12 ± 0.16	7.29 ± 0.11
cNLC6	4.09 ± 0.26	7.22 ± 0.07

[a] For the compositions of cSLNs and cNLCs see **Table 1** and **Table 2**, respectively.

The results are expressed as mean ± SD of three measurements.